CT-Like Images from MRI: A Comprehensive Review of the Zero-Echo-Time Sequence

Yesim Yekta Yuruk, MD; Mehmet Simsar, MD; Yeliz Pekcevik, MD

MRI is a noninvasive imaging modality that provides excellent soft-tissue contrast and high resolution of anatomic detail in the body structures without ionizing radiation.[1,2] Despite these advantages, conventional MRI sequences are not as successful as CT in depicting the bone cortex and calcified structures owing to these structures' low proton density (approximately 20% water) and short T2 relaxation times (approximately 390milliseconds at 3 T MRI).[3]

CT is more successful in imaging bone structures and calcifications, owing to the modality's high spatial resolution, fast acquisition, and high availability. However, poor soft-tissue resolution and radiation exposure are the major disadvantages of CT.[4,5]

Therefore, MRI may be a more ideal modality if better cortical bone and calcific structure image quality are provided. This is possible with the zero-echo-time (ZTE) MRI sequence, a new technique that uses ultra-fast readouts to capture signals from short-T2 tissues and aims to capture cortical bone and calcific structure images without ionizing radiation. This sequence provides "CT-like" images with the additional benefits of fast scan time, silent scanning, and artifact resistance.[6-10]

Imaging Technique of the ZTE Sequence

The basis of the ZTE sequence is to focus on very short T2 time tissues and structures considered invisible on MRI. The bone cortex and calcified structures have low proton density and short T2 relaxation times.[3] Therefore, the appearance of these structures results in signal voids on conventional MRI sequences.

The ZTE sequence is based on nonselective volume excitation and 3D radial center-out k-space encoding. Gradients are used continuously, and progressively reorienting in the x, y, and z axes between repetitions. Thus, the data are sampled along purely frequency-encoded center-out 3D radial trajectories in k-space (Figure 1).[11,12]

The acquisition of the free induction decay signal occurs immediately after excitation. The fast radiofrequency (RF) switch from transmit to receive enables acquisition of the quickly decaying signal starting at near-zero-echo time. The principle of capturing the small amount of signal found in cortical bone and calcific structures is based on this MRI physics.

In contrast to conventional pulse sequences, ZTE utilizes a readout gradient amplitude that is kept consistent throughout scanning with small directional changes between repetitions. This method outputs unique properties regarding silent scanning and nominal zero echo time.[12]

In ZTE, the RF excitation is entangled with the image encoding readout gradient. The RF block pulses are able to achieve consistent excitation because the RF excitation bandwidth covers the full RF imaging bandwidth, regardless of the readout gradient. As a result, the RF pulse width must be shorter than the RF sampling period, thereby limiting the maximum possible flip angle. If the RF pulse width is longer than the RF sampling period, the readout gradient may cause sinc-shape modulation of the RF excitation profile along the readout direction. Owing to the changing readout direction throughout the sequence, this would cause blurring that scales with increasing distance from the center of the imaging field of view (FOV).[13]

Chemical shift artifacts lead to image blurring and signal interference at fat-water interfaces, thus degrading the clarity of cortical bone depiction. To prevent this

Affiliations: Department of Radiology, Izmir Tepecik Education and Research Hospital, University of Health Sciences, Izmir, Turkey (Yuruk). Department of Radiology, Izmir City Hospital, Izmir, Turkey (Yuruk, Simsar, Pekcevik). Department of Radiology, Izmir Faculty of Medicine, University of Health Sciences, Izmir, Turkey (Pekcevik).

Disclosure: The authors have no conflicts of interest to disclose. None of the authors received outside funding for the production of this original manuscript and no part of this article has been previously published elsewhere.

Published: February 1, 2025. https://doi.org/10.37549/AR-D-24-0065

Figure 1. Illustration of zero-echo-time sequence. Gradients (G) are ramped up before the initial radiofrequency (RF) pulse. Gradients are continuously on with modulations prior to individual RF excitations and switched off at the end of the sequence. As a result of the dead-time (Δt) following the RF (while the signal cannot be acquired), there is a spherical gap at the center of the k-space, resulting in the missed data points.

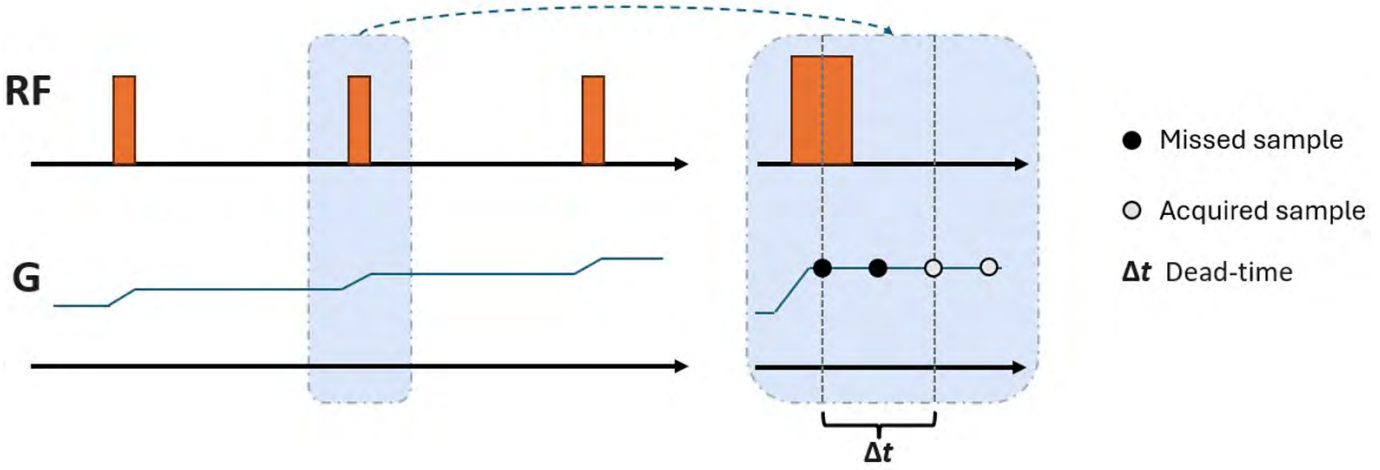

degradation, a pixel bandwidth larger than the oil-water chemical shift (i.e., 3.5 ppm) should be used.[13]

Robust coil bias correction along with grayscale inversion may assist in differentiating cortical bone from other short-T2, collagen-rich structures (the joint capsule, labra, or menisci) by producing CT-like images. Another advantage of the ZTE is that it allows the use of intensity projection to produce CT-like images and multiplanar and radial reformatting as in CT. The spatial resolution of ZTE is lower than that of CT. Today, the spatial resolution of ZTE is 0.8-1.2 cm, while the current highest value of CT is 0.625 mm. Despite the low spatial resolution of ZTE, CT-like images may be obtained by grayscale inversion automatically or with a single click via the picture archiving and communication system.[13-15]

Ultimately, several factors play a role in determining the usability of ZTE images for clinical purposes. Of these factors, receiver bandwidth (50 kHz at 1.5 T and 62.5 or 83.33 kHz at 3 T), flip angle (1° or 2°), and FOV (180 × 180 mm through 420 × 420 mm) are particularly important.[13] Knowing all these imaging features allows for better-quality images to be obtained.

Clinical Feasibility of the ZTE Sequence

Musculoskeletal Imaging

Computed tomography and radiography are often used to evaluate bone and calcific structures, while MRI is typically used to evaluate soft tissues such as muscles and tendons (Figure 2). Radiography or CT is used when conventional MRI is unable to distinguish pathology from bone and soft tissue. In addition, diagnosis may be difficult in cases where the patient has not had previous CT or radiography (Figure 3).

MRI, which includes the ZTE sequence, provides great benefit in terms of clinical use as it displays bone tissue and calcifications along with soft tissues (Figure 4).[3,6] With this method, many pathologies such as rheumatoid arthritis, osteoarthritis, spondylolysis, spondylolisthesis, fracture, joint dislocation, and metastases can be diagnosed with MRI instead of CT.[10,16] Moreover, MRI with the ZTE sequence is especially useful in cases where radiation should be avoided, such as in children, pregnant women, and patients with cancer.[17,18]

Head and Neck Imaging

Despite the increasing use of ZTE in musculoskeletal and body imaging, neuroimaging applications have been limited by the complexity of the head and neck anatomy and pathology.[19,20] Therefore, using the ZTE sequence in the head and neck is generally limited to acute trauma, pediatric patients, pregnant patients, metastasis screening, craniofacial malformations, and patients with genetic disorders who should not be exposed to radiation (Figure 5).[19]

Apart from these exceptions, there are examples in the literature that use MR angiography (MRA) with the ZTE sequence. ZTE imaging can be used in conjunction with an arterial spin labeling preparation module to achieve higher contrast during MRA.[21] ZTE-MRA may reduce artifacts around areas of magnetic

Figure 2. Sagittal plane x-ray image (A), zero-echo-time (ZTE)-grayscale inversion (B), T2 (C), and ZTE (D) MRI images from a normal left ankle. In ZTE-MRI, cortical bone structures are better demarcated and evaluated to the T2 sequence and are more like radiography.

Figure 3. Coronal plane T1 (A), zero-echo-time (ZTE)-grayscale inversion (B), and ZTE (C) MR images from the normal bilateral hip joints. In ZTE, the joint structure, acetabular roof, and cortical bone structures are evaluated more clearly compared with conventional MRI sequences.

Figure 4. Coronal plane T1 (A) and axial plane proton density (B) images demonstrate a thickness in the supraspinatus tendon at the level of its attachment to the humerus (arrows). Zero-echo-time-grayscale inversion (C) MR image clearly shows calcifications within the thickened tendon (arrowhead).

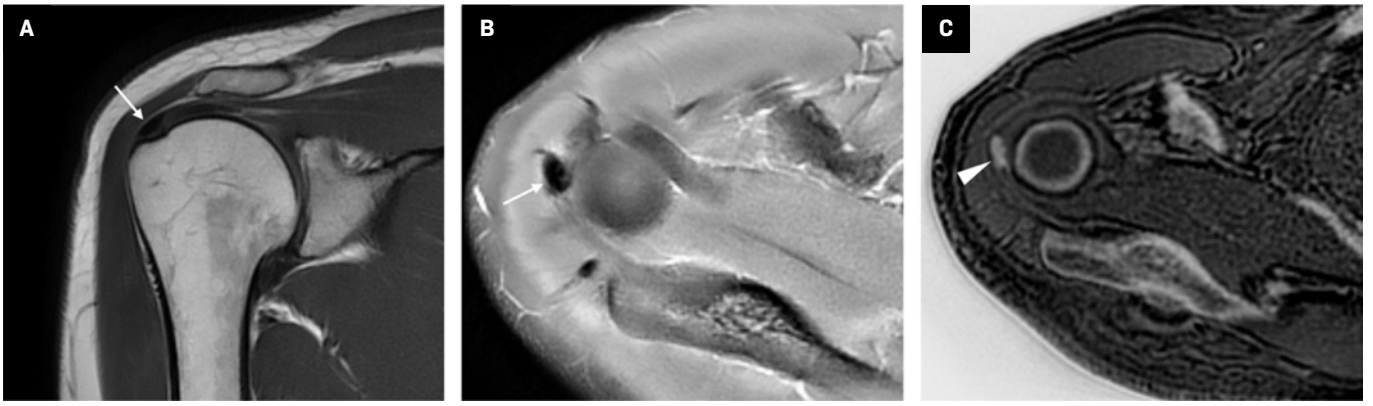

Figure 5. Axial (A) and coronal plane T1 (D) MR images show a low-signal lesion adjacent to the left mandible ramus (arrows). Axial (B) and coronal plane (E) zero-echo-time (ZTE)-grayscale inversion images show that the lesion originates from the ramus of the mandible. Axial (C) and coronal plane CT (F) images show similar features to the ZTE images and clearly show that the mass originates from the mandibular ramus. The lesion was diagnosed as an osteoma.

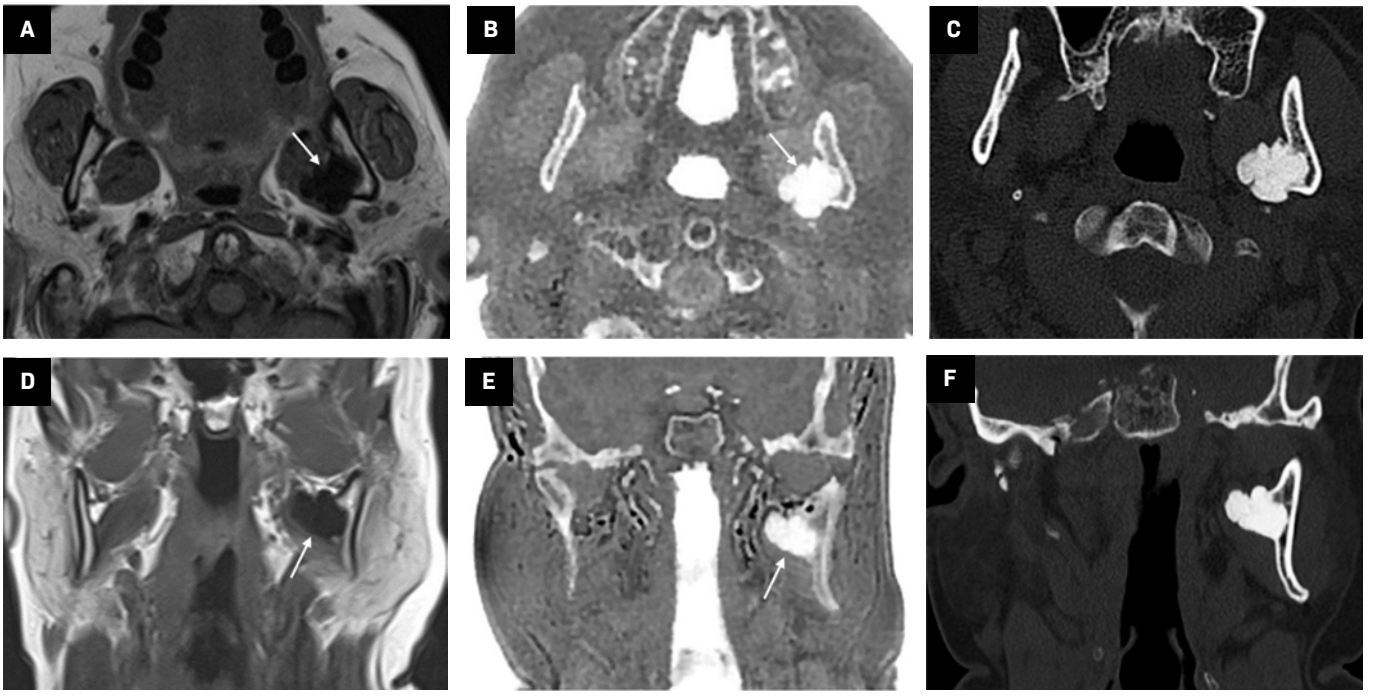

susceptibility gradients, which is important for imaging around stents and coils. Several studies have demonstrated improved vessel visualization around stents and coils with ZTE-MRA compared with conventional gradient echo-based TOF-MRA.[22-25]

Pediatric Imaging

Because it can image bone and soft-tissue pathologies without ionizing radiation, ZTE-MRI is expected to increase in popularity in pediatric imaging (Figure 6). Indeed, it is beginning to be used in some centers to image for suspected pathologies such as renal stones, ureteral stones, and bladder stones.[18]

Lung Imaging

Although high-resolution CT is primarily used for lung imaging, MRI with the ZTE sequence is being used

Figure 6. A 1-year-old with left-leg swelling. x-ray (A) shows a periosteal reaction at the lower end of the femur (arrows). However, no bone lesion could be distinguished on x-ray. Zero-echo-time-grayscale inversion (B) MR images clearly demonstrate a lytic bone lesion (arrowhead). The lesion was diagnosed as osteomyelitis.

Figure 7. Coronal plane zero-echo-timeMRI lung image.

in some centers as a radiation-free imaging method to diagnose and manage cystic fibrosis (Figure 7). MRI has the unique ability to distinguish scar tissue from active inflammation, making it particularly useful in this condition.[25]

Conclusion

The ZTE MRI sequence is a new technique that uses ultra-fast readouts to capture signals from short-T2 tissues to image cortical bone and calcific structures without ionizing radiation. This presents significant advantages over CT in pediatric patients, pregnant persons, and metastasis screening. It also represents a significant alternative to CT owing to its rapid screening speed, silent scanning, and artifact resistance. All-in-one MRI, including "CT-like images," appears poised to be used increasingly more often in the near future.

References

1) Lauterbur PC. Image formation by induced local interactions: examples employing nuclear magnetic resonance. *Nature*. 1973;242(5394):190-191. doi:10.1038/242190a0

2) Mansfield P. Multi-planar image formation using NMR spin echoes. *J Phys C: Solid State Phys*. 1977;10(3):L55-L58. doi:10.1088/0022-3719/10/3/004

3) Du J, Carl M, Bydder M, et al. Qualitative and quantitative Ultrashort Echo Time (UTE) imaging of cortical bone. *J Magn Reson*. 2010;207(2):304-311. doi:10.1016/j.jmr.2010.09.013

4) Zeman RK, Fox SH, Silverman PM, et al. Helical (spiral) CT of the abdomen. *AJR Am J Roentgenol*. 1993;160(4):719-725. doi:10.2214/ajr.160.4.8456652

5) Mettler FA Jr, Bhargavan M, Faulkner K, et al. Radiologic and nuclear medicine studies in the united states and worldwide: frequency, radiation dose, and comparison with other radiation sources—1950-2007. *Radiology*. 2009;253(2):520-531. doi:10.1148/radiol.2532082010

6) Wiesinger F, Sacolick LI, Menini A, et al. Zero TE MR bone imaging in the head. *Magn Reson Med*. 2016;75(1):107-114. doi:10.1002/mrm.25545

7) Endo Y. Diagnostic accuracy of zero-echo time MRI for the evaluation of cervical neural foraminal stenosis. *Spine*. 1976;43(13):928-933. doi:10.1097/BRS.0000000000002462

8) Breighner RE, Endo Y, Konin GP, et al. Technical developments: zero echo time imaging of the shoulder: enhanced osseous detail by using MR imaging. *Radiology*. 2018;286(3):960-966. doi:10.1148/radiol.2017170906

9) Breighner RE, Bogner EA, Lee SC, Koff MF, Potter HG. Evaluation of osseous morphology of the hip using zero echo time magnetic resonance imaging. *Am J Sports Med*. 2019;47(14):3460-3468. doi:10.1177/0363546519878170

10) Cho SB, Baek HJ, Ryu KH, et al. Clinical feasibility of zero TE skull MRI in patients with head trauma in comparison with CT: a single-center study. *AJNR Am J Neuroradiol*. 2019;40(1):109-115. doi:10.3174/ajnr.A5916

11) Weiger M, Pruessmann KP, Hennel F. MRI with zero echo time: hard versus sweep pulse excitation. *Magn Reson Med*. 2011;66(2):379-389. doi:10.1002/mrm.22799

12) Mastrogiacomo S, Dou W, Jansen JA, Walboomers XF. Magnetic resonance imaging of hard tissues and hard tissue engineered bio-substitutes. *Mol Imaging Biol*. 2019;21(6):1003-1019. doi:10.1007/s11307-019-01345-2

13) Aydıngöz Ü, Yıldız AE, Ergen FB. Zero echo time musculoskeletal MRI: technique, optimization, applications, and pitfalls. *Radiographics*. 2022;42(5):1398-1414. doi:10.1148/rg.220029

14) Froidevaux R, Weiger M, Rösler MB, Brunner DO, Pruessmann KP. HYFI: hybrid filling of the dead-time gap for faster zero echo time imaging. *NMR Biomed*. 2021;34(6):e4493. doi:10.1002/nbm.4493

15) Ilbey S, Jungmann PM, Fischer J, et al. Single point imaging with radial acquisition and compressed sensing. *Magn Reson Med*. 2022;87(6):2685-2696. doi:10.1002/mrm.29156

16) Bessa FS, Williams BT, Polce EM, et al. No differences in hip joint space measurements between weightbearing or supine anteroposterior pelvic radiographs. *Arthroscopy*. 2020;36(11):2843-2848. doi:10.1016/j.arthro.2020.07.009

17) Larson PEZ, Han M, Krug R, et al. Ultrashort echo time and zero echo time MRI at 7T. *MAGMA*. 2016;29(3):359-370. doi:10.1007/s10334-015-0509-0

18) Ozcan HN, Ozer G, Dogan HS, et al. Zero-echo time MRI: an alternative method for the diagnosis of urinary stones in children. *Eur Radiol*. 2025;35(1):289-296. doi:10.1007/s00330-024-10950-x

19) Wiesinger F, Ho M-L. Zero-TE MRI: principles and applications in the head and neck. *Br J Radiol*. 2022;95(1136):20220059. doi:10.1259/bjr.20220059

20) Zheng W, Kim JP, Kadbi M, et al. Magnetic resonance-based automatic air segmentation for generation of synthetic computed tomography scans in the head region. *Int J Radiat Oncol Biol Phys*. 2015;93(3):497-506. doi:10.1016/j.ijrobp.2015.07.001

21) Shang S, Ye J, Dou W, et al. Validation of zero TE-MRA in the characterization of cerebrovascular diseases: a feasibility study. *AJNR Am J Neuroradiol*. 2019;40(9):1484-1490. doi:10.3174/ajnr.A6173

22) Irie R, Suzuki M, Yamamoto M, et al. Assessing blood flow in an intracranial stent: a feasibility study of MR angiography using a silent scan after stent-assisted coil embolization for anterior circulation aneurysms. *AJNR Am J Neuroradiol*. 2015;36(5):967-970. doi:10.3174/ajnr.A4199

23) Takano N, Suzuki M, Irie R, et al. Non-contrast-enhanced silent scan MR angiography of intracranial anterior circulation aneurysms treated with a low-profile visualized intraluminal support device. *AJNR Am J Neuroradiol*. 2017;38(8):1610-1616. doi:10.3174/ajnr.A5223

24) Shang S, Ye J, Luo X, et al. Follow-up assessment of coiled intracranial aneurysms using ZTE MRA as compared with TOF MRA: a preliminary image quality study. *Eur Radiol*. 2017;27(10):4271-4280. doi:10.1007/s00330-017-4794-z

25) Heo YJ, Jeong HW, Baek JW, et al. Pointwise encoding time reduction with radial acquisition with subtraction-based MRA during the follow-up of stent-assisted coil embolization of anterior circulation aneurysms. *AJNR Am J Neuroradiol*. 2019;40(5):815-819. doi:10.3174/ajnr.A6035